Langmuir

Article

pubs.acs.org/Langmuir

Use of Ultrasound Attenuation Spectroscopy to Determine the Size Distribution of Clay Tactoids in Aqueous Suspensions

Samim Ali* and Ranjini Bandyopadhyay*

Raman Research Institute, C. V. Raman Avenue, Sadashivanagar, Bangalore 560080, India

Supporting Information

ABSTRACT: The dispersion processes of aqueous samples of clay are studied using ultrasound attenuation spectroscopy. The attenuation spectra that are acquired in the frequency range 10−100 MHz are used to determine the particle size distributions (PSDs) for different concentrations and ages of the clay suspensions. Our analysis, using equivalent spherical diameter (ESD) for circular discs under Stokes drag in samples of concentrations greater than 1.5% w/v, shows that a substantial fraction of the aggregates in suspension are actually tactoids that are composed of more than one platelet. This is in contrast to the general belief that clay disperses into individual platelets in the concentration range where their suspensions exhibit glassy behavior. We conclude that the incomplete fragmentation of the clay tactoids arises from the rapid enhancement of the intertactoid Coulombic repulsion.

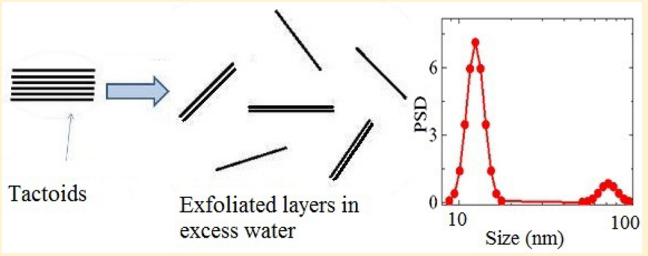

I. INTRODUCTION

Laponite is a synthetic Hectorite clay whose aqueous suspensions have often been used in the study of the glass transition phenomenon. A single Laponite platelet has a thickness of 1 nm and a diameter of 25−30 nm.[1] Because of the highly anisotropic shape and the large negative charges on the flat surfaces, Laponite clays in aqueous suspensions can exhibit a spontaneous ergodicity-breaking phase transition from free-flowing liquids to nonequilibrium, kinetically arrested states such as gels and glasses at low concentrations (0.5%−4%).[2] Due to the nonequilibrium nature of these arrested states, they exhibit aging, with the dynamic and thermodynamic properties of these suspensions evolving as the waiting time (measured from immediately after the time of preparation) increases. Aging in these systems occurs by the spatially and temporally correlated local rearrangements of particles that can overcome local energy barriers, with the system exploring progressively deeper energy wells in phase space.[3] The different arrested phases exhibit viscoelastic properties under different applied stress−strain conditions. On application of stresses above a yield value, the elastic and viscous moduli of these soft solids decrease and the suspensions eventually flow like a fluid. Once the applied stress is removed, the suspension gradually recovers its jammed state.[4] Besides their obvious importance in fundamental research, aqueous suspensions of Laponite also find wide applications in the petroleum, cosmetics, pharmaceutical, coating, and food industries.[5,6]

It is believed that a major factor contributing to the time-dependent behavior of aqueous suspensions is the swelling and subsequent breakup of large Laponite clusters into smaller entities.[7] Due to the importance of Laponite suspensions in various technological processes and their frequent use as model glass formers, the dispersion kinetics of Laponite clay under different experimental conditions needs to be studied. In most of the studies undertaken previously, clusters of clay particles were assumed to exfoliate into individual platelets when dispersed in water. However, several studies also show that clay particles can exist as rigid aggregates, known as tactoids, that consist of more than one platelet oriented in parallel. Many experimental methods [e.g., atomic force microscopy (AFM), transmission electron microscopy (TEM), cryogenic scanning electron microscopy (Cryo-SEM), small angle X-ray scattering (SAXS), small angle neutron scattering (SANS), dynamic light scattering (DLS), and transient electrically induced birefringence (TEB)] have been employed to characterize the tactoid sizes of clays in aqueous suspensions at different concentrations and under varying experimental conditions.[8−13] However, a systematic study of the particle size distribution (PSD) in aqueous clay suspensions and its dependence on the clay volume fraction and suspension age is still lacking. Indeed, DLS has been used intensively for particle sizing, but its application is limited to very dilute suspensions where the single scattering mechanism and the Stokes−Einstein relation are valid. Several DLS studies show a sol−glass transition with increase in concentration and age of the clay suspensions.[14−17] Intensity autocorrelation data obtained in DLS experiments is typically analyzed in terms of a fast (τ_1) and a slow relaxation time (τ_2).[18] However, it is very difficult to acquire PSD information from τ_1 and τ_2 in the glassy phase as the Stokes−Einstein relation is invalid.

Received: July 1, 2013
Revised: September 16, 2013
Published: September 17, 2013

The aim of this paper is to investigate the dispersion of Laponite clay in aqueous suspensions of different ages using ultrasound attenuation spectroscopy (UAS). The UAS techniques offer a unique possibility of estimating PSDs for soft solid systems and can be used to analyze nontransparent and even highly structured systems. At the same time, it is a nondestructive technique that uses very low intensity ultrasound. The measurement does not, therefore, affect the sample microstructures and yields an accurate estimate of average particle sizes and PSDs. Over the last two decades, this technique has been applied in different particulate systems of quartz, rutile, latex, alumina particles, and also in emulsions.[19] In this work, we measure ultrasound attenuation spectra to estimate PSDs of clay tactoids in Laponite suspensions in the concentration range (1.5%−4% w/v) where the suspensions spontaneously show liquid to soft solid transitions with increasing age. Furthermore, AFM data has been acquired to confirm the average platelet sizes of both Laponite and Na-montmorillonite particles in aqueous suspension. We show here that the dispersion kinetics of both clay suspensions follow the same approximate trends.

II. MATERIALS AND METHODS

A. Material Structure and Sample Preparation. Two different smectite clays: Laponite and Na-montmorillonite are investigated in this study. Both clays are from the phyllosilicate group with a 2:1 structure, in which an octahedral metal sublayer is sandwiched between two tetrahedral silica sublayers. The three sublayers together form a single unit crystal layer which grows in lateral direction to form a platelet or sheet structure. Some of the metal ions (magnesium in Laponite and aluminum in Na-montmorillonite) in the octahedral sublayer get replaced isomorphically by lower valency ions (lithium and magnesium, respectively, for the two clays). This results in negative charges on the outer surface without any structural change. The rim of the platelet gains positive charges due to the protonation of the OH^- group below a suspension pH of 10. In the dry powder form, the van der Waals interactions between unit layers lead to the stacking of platelets with intercalated sodium counterions. These stacks of clay platelets are known as tactoids. Laponite is a highly pure variety of synthetic clay with a very reproducible chemical composition. In accordance with the manufacturer, the thickness of a Laponite platelet is approximately 1 nm, while its diameter is in the range of 25−30 nm. The thickness and diameter ranges of individual Laponite platelets, verified using atomic force microscopy (AFM), are shown in Figures S1 and S2 of the Supporting Information. Na-montmorillonite is a natural clay sourced from volcanic ash. The thickness of the Na-montmorillonite platelet is approximately 1 nm, while its lateral size may vary from a few nanometers to several micrometers. Laponite of RD grade (mass density of 2.53 g/cm^3) is purchased from Southern Clay Products, and Na-montmorillonite (mass density 2.60 g/cm^3) is procured from Nanocor Inc. Clay powder is heated in an oven at a temperature of 120 °C for 24 h before it is dispersed in highly deionized Milli-Q water under vigorous stirring conditions. The powder is added very slowly and in very small amounts to avoid the formation of large aggregates, following which the suspension is stirred vigorously for 45 min using an IKA Turrex drive to ensure a homogeneous distribution of the aggregates.

B. Acoustic Spectroscopy: Theory and Measurements. The propagation of sound waves through a medium is closely related to its rheological and acoustic properties.[20] The crucial rheological parameters are the bulk elastic modulus M and the dynamic viscosity η, while the basic acoustic parameters are the attenuation coefficient α and the sound speed c. Ultrasound spectroscopy measures the attenuation of acoustic waves of MHz frequency by the medium. In this technique, the elastic and dissipative characteristics of the medium are combined into a single complex parameter k, the "compression complex wavenumber". α and c are related to k as follows:[19]

$$\alpha = -Im(k) \tag{1}$$

$$c = \frac{\omega}{Re(k)} \tag{2}$$

Here, ω is the angular frequency of the ultrasound waves and α is closely related to the sizes and distributions of the colloidal particles in the suspension medium. When ultrasound interacts with a colloidal sample, dissipation can occur due to a combination of viscous, thermal, scattering, intrinsic, structural, and electrokinetic processes. If the ultrasound wavelength λ is larger than the particle size a, α can be written as a sum of the different loss mechanisms, $\alpha = \alpha_{vis} + \alpha_{th} + \alpha_{sc} + \alpha_{int}$, where α_{vis}, α_{th}, α_{sc}, and α_{int} are the contributions of the viscous, thermal, scattering, and intrinsic mechanisms, respectively. The contributions from structural and electrokinetic losses are typically negligible for particulate systems and have not been included here. With dependence on the nature and concentration of the colloidal particles under study, it may be possible to separate the different loss mechanisms in the ultrasound frequency domain. In the frequency range of 1−100 MHz, the viscous loss mechanism dominates, as the aqueous suspensions used here are characterized by high particle density contrasts and rigidities. As the frequency changes from 1 to 100 MHz, the wavelength of ultrasound in water changes from 1 mm to 15 μm. Scattering loss is negligible as the wavelength range of ultrasound is much larger than the expected sizes of the particles. The expression for the complex wavenumber k, derived in ref 19 on the basis of the coupled phase model,[21,22] by assuming a predominantly viscous loss in the long wavelength limit ($ka \ll 1$) can be written as

$$\frac{k^2M^*}{\omega^2\rho_s} = \frac{1 - \frac{\rho_p}{\rho_s}\sum_{i=1}^{N}\frac{\phi_i}{1-(9j\rho_m\Omega_i/4s_i^2\rho_p)}}{1 + \left(\frac{\rho_s}{\rho_p} - 2\right)\sum_{i=1}^{N}\frac{\phi_i}{1-(9j\rho_m\Omega_i/4s_i^2\rho_p)}} \tag{3}$$

where

$$s_i^2 = \frac{a_i^2\omega\rho_m}{2\eta_m} \tag{4}$$

$$\rho_s = \rho_p\phi + \rho_m(1-\phi) \tag{5}$$

and

$$M^* = \frac{\rho_p\rho_m c_p^2 c_m^2}{\phi\rho_p c_p^2 + (1-\phi)\rho_m c_m^2} \tag{6}$$

Here, M^* is the stress modulus, ρ_p is the density of the particle, ρ_m is the density of the medium, ρ_s is the density of the suspension, ϕ_i is the volume fraction of the ith species of the particulate phase, ϕ is the total volume fraction of the particulate phase, a_i is diameter of a particle of the ith species, η_m is the shear viscosity of the medium, and Ω_i is the drag

dx.doi.org/10.1021/la402478h | Langmuir 2013, 29, 12663−12669

coefficient of a particle of size a_i. The Happel cell model is used to incorporate hydrodynamic interactions between the particles.[19,23] When eqs 3−6 are coupled with eqs 1 and 2, α and c can be measured.

In a typical experiment, if the incident sound intensity is I_0 and the attenuated intensity after passing through a sample of length x is I_x, then the Beer−Lambert law gives an expression for the attenuation coefficient α of the medium:[24]

$$\alpha = \frac{10}{x}\log\frac{I_0}{I_x} \tag{7}$$

Here α is usually expressed in dB cm^{-1} and depends on the acoustic frequency (ω). This law can easily be verified for the colloidal systems studied in this work (Figure S3 of the Supporting Information shows data for a 3% w/v Laponite suspension). The measurements of attenuation coefficients α at varying frequencies give an attenuation spectrum, which can be fitted with the theoretical prediction (eq 3), using the supplied values of ρ_m, η_m, ρ_p, c_p, and ϕ (details are provided in the Supporting Information).

In this work, the attenuation spectra and sound speed are measured using a DT-1200 acoustic spectrometer from Dispersion Technology Inc. Details of this spectrometer can be found in ref 19. For each attenuation measurement, 130 mL of the clay suspension is loaded in a cell containing two identical piezoelectric transducers separated by a gap of 20 mm. The transmitting transducer converts input electrical signals into ultrasound tone bursts of different intensities and frequencies. The ultrasound pulse that is generated propagates through the suspension and interacts with the colloidal particles and the liquid medium (water). This interaction decreases the ultrasound intensity, with the predominant loss mechanisms being the viscous loss of the colloids and the intrinsic loss of water. The intensity amplitude of the pulse, received by the detecting transducer, is converted back into an electric pulse for comparing with the initial input pulse. For each frequency, the signal processor receives data for a minimum of 800 pulses to achieve a signal-to-noise ratio of at least 40 dB. The intrinsic loss contribution is subtracted from the total intensity loss to estimate the attenuation arising from the colloids alone. The sound pulses used here are of low power (250 mW) and are not expected to destroy the microscopic structures of the suspensions. The sound speed c is obtained by measuring the time delay between the emitted and received pulses.

The attenuation spectra are measured for different ages, t_w, of the colloidal suspensions by varying the ultrasound frequency in the range from 10 to 99.5 MHz with 18 logarithmic steps. t_w = 0 is defined as the time at which the stirring of the sample is stopped. The sample is kept undisturbed during the whole experimental time to prevent destruction of the jammed structures that form as the suspension ages. Prior to these experiments, the sample cell is calibrated for acoustic diffraction using Milli-Q water. All the experiments reported here are performed at 25 °C.

An analysis algorithm, developed by the manufacturer and based on the theory described earlier, is used to determine the PSD from attenuation spectra. The algorithm, assuming unimodal or bimodal distributions, runs a search in the size range from 1 nm to 1 mm for the PSD that best fits the data. For a unimodal (log-normal) distribution, the median and the standard deviation of the particle sizes are the fitting parameters. For a bimodal PSD, essentially a sum of two log-normal PSDs, the algorithm adjusts four parameters: the two median values (d_1 and d_2) of the lower and higher modes, their standard deviation (assumed to be of the same magnitude σ for both modes), and the relative volume fraction (ϕ_2) of particles in the higher mode. During the search process, the algorithm calculates the theoretical attenuation values for each PSD using eqs 1 and 2 and fits the experimental attenuation spectrum by minimizing the fitting error. The searching algorithm stops when the fitting error saturates to the lowest value. The algorithm performs very well for many standard spherical particles (e.g., Ludox TM50[19] and Silica Koestrosol 1530[25]). In this work, acoustic measurements are performed on Laponite clay suspensions in a concentration range between 1.5% and 4% w/v and in 1% w/v Na-montmorillonite suspensions.

C. Rheology. Rheological measurements are carried out at 25 °C with a stress-controlled rheometer (Anton Paar MCR 501) using a Couette geometry. The sample preparation protocol for rheological measurements are the same as that for the acoustic measurements. For each test, a sample volume of 4.7 mL is loaded in the sample cell just after preparation and is presheared using a high shear stress (60 Pa at an angular frequency ω of 10 rad/s) for one minute to achieve a reproducible starting point for the aging experiments. The aging process is monitored by recording the evolution of the elastic modulus G' and the viscous modulus G'' with aging time t_w, when an oscillatory strain of amplitude γ_0 = 0.5% and angular frequency ω = 1 rad/s is applied.

D. AFM Measurements. A drop of 10 μL sample is deposited on a freshly cleaved mica surface (area of 1 cm^2) and allowed to dry in a closed Petri dish under ambient conditions. The AFM micrographs are obtained using a PicoPlus scanning probe microscope (Molecular Imaging Company) operated in tapping or contact mode. In the tapping mode, a cantilever of dimension 225 μm × 38 μm × 7 μm with a tip height of 10 μm oscillates at its resonant frequency, which in air has a value of 146−236 kHz. In the contact mode, a cantilever of dimension 450 μm × 50 μm × 2 μm with a tip height of 10 μm is used. Data acquisition and size analysis are done using PicoScan 5.3.3 supplied by Molecular Imaging Company.

III. RESULTS AND DISCUSSION

Figure 1 shows the measured attenuation spectrum (□) for a 3% w/v Laponite suspension of age t_w = 6 h and the two theoretical fits for unimodal and bimodal PSDs (dashed and solid lines, respectively). The fitting errors obtained are 3.6% for the unimodal distribution and 1.3% for the bimodal distribution. The PSDs obtained from the two fits are plotted in the inset of Figure 1 and can be seen to differ substantially.

As a clay platelet is anisotropic, the viscous loss is dependent on its orientation relative to the sound propagation direction. A disc moving edgewise causes greater viscous loss than a disc moving broadside.[26,27] The theory discussed above considers the dispersed particles as spheres. The theoretical fits to the experimental data therefore yields an equivalent spherical diameter (ESD), d_s, which can be related to the platelet dimension using the Jennings−Parslow relation for anisotropic particle under Stokes drag:[28]

$$d_s = d\left[\frac{3}{2}\frac{\arctan\sqrt{\left(\frac{d}{t}\right)^2 - 1}}{\sqrt{\left(\frac{d}{t}\right)^2 - 1}}\right]^{1/2} \tag{8}$$

dx.doi.org/10.1021/la402478h | Langmuir 2013, 29, 12663−12669

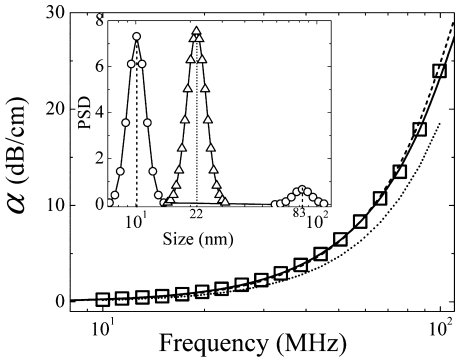

Figure 1. The attenuation spectrum (□) for a 3% w/v Laponite suspension at t_w = 6 h. The dashed and solid lines are theoretical fits, considering unimodal and bimodal size distributions, respectively. The dotted line corresponds to the intrinsic attenuation in pure water. The unimodal and bimodal particle size distributions (PSDs) obtained from the theoretical fits to the attenuation spectrum are plotted in the inset with △ and ○, respectively.

Here, d and t are the diameter and thickness of the disc, respectively.

The inset of Figure 1 shows that the unimodal fit (△) to the attenuation curve has a median particle size value of 22 nm. As the basic Laponite platelet is known to be very regular in shape and size, with platelet diameter 25−30 nm and thickness of 1 nm,[29] it is possible to estimate the thickness t of a tactoid from d_s by using eq 8. With consideration of a one-dimensional stack of platelets, the optimum graphical solution of eq 8 (shown in Figure 2) gives a disc diameter d of 25−30 nm with a thickness

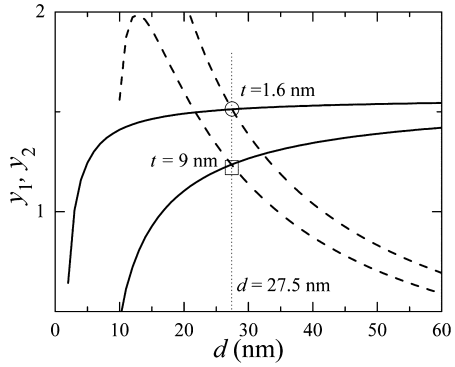

Figure 2. The graphical solutions of eq 8 for different ESDs. The solution for the median size (d_s = 22 nm) obtained in the unimodal fit corresponds to a Laponite disc of diameter 25−30 nm, when its thicknesses is t = 9 nm (indicated by a square). For the bimodal fit, a median size d_1 = 10 nm is obtained for the lower mode. This corresponds to a disc thickness of t = 1.6 nm (indicated by a circle). Here, $y_1 = \arctan[(d/t)^2 - 1]^{1/2}$, is plotted using solid lines and $y_2 = (2/3)(d_s^2/d^2)[(d/t)^2 - 1]^{1/2}$ is plotted using dashed lines.

of t = 9 ± 1 nm. As the thickness of a single platelet is 1 nm, this indicates that the majority of the tactoids in suspension are composed of 9 platelets. On the other hand, the bimodal fit (○ in Figure 1) gives two median values: d_1 = 10 nm for the lower mode and d_2 = 83 nm for the higher mode, with the relative concentration ϕ_2 for the higher mode being around 10%. The graphical solution of eq 8 (shown in Figure 2), d_s = 10 nm, corresponding to the lower mode of the bimodal fit, implies a thickness of t = 1.6 ± 0.15 nm for a disc diameter of d = 25−30 nm. The bimodal assumption is therefore reasonable and confirms earlier reports that claimed the existence of very small Laponite tactoids in suspensions.[8−11] The spread in the lower mode of the bimodal PSD indicates a size polydispersity and implies that tactoids with more than one platelet are also present in suspension. Further details of the graphical solutions can be found in the Supporting Information.

The contribution to the higher mode of the bimodal distribution (inset of Figure 1), with a median value (d_2) of 80 nm, is believed to be from larger aggregates and from a very small number of unavoidable bubbles. We should point out here that there is a fair possibility of the incomplete disintegration of some of the clay clusters in the aqueous medium.[30] The presence of small fractions of larger aggregates has also been shown in some previous studies (e.g., in electro-optical experiments on 0.01 wt % Laponite suspensions).[31] We therefore believe that modeling the aggregate size distribution with a bimodal function is a better choice than the unimodal function, as the former can efficiently separate the contribution of the big aggregates.

Ultrasound attenuation measurements have also been performed in aqueous suspensions of another anisotropic colloidal clay, Na-montmorillonite, to verify the techniques already described. Compared to Laponite, Na-montmorillonite clay particles are more polydisperse in size and have irregular edge boundaries.[32] The attenuation spectrum and the aggregate size distribution of a 1% w/v Na-montmorillonite suspension of age t_w = 17 days are shown in Figure 3. As the clay

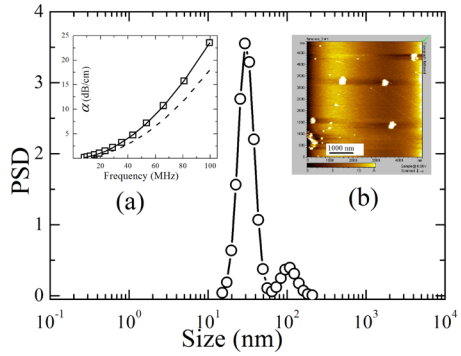

Figure 3. The bimodal size distribution of aggregates of a 1% w/v Na-montmorillonite suspension at t_w = 17 days. The corresponding attenuation spectrum (attenuation coefficient α vs ultrasound frequency) is denoted by squares in the inset (a). The solid line in the inset (a) is the theoretical fit considering the bimodal distribution, while the dotted line denotes the intrinsic attenuation spectrum in pure water. An AFM image of Na-montmorillonite sheets (white patches) is shown in inset (b). The scan size is 5 μm × 5 μm.

concentration is low and the sample is stirred vigorously for several days, we assume that a substantial part of clay aggregates are exfoliated into tactoids comprising one to two platelets. In consideration of a bimodal PSD, the theoretical prediction of the attenuation [shown by the solid line in the inset (a) of Figure 3] fits well to the experimental results (with a fitting error of 1.5%) to yield d_1 = 30.1 nm, d_2 = 105 nm, and ϕ_2 = 13%. The lower mode, d_1 = 30.1 nm, gives an equivalent plate diameter of d = 254 nm and a thickness of t = 1.5 nm (graphical solution of eq 8 is plotted in Figure S4 of the Supporting Information). AFM images of the same sample are shown in the inset (b) of Figure 3. An average size measurement (see Figures S5 and S6 of the Supporting Information) of clay sheets yields an average particle diameter of d = 282 ± 30 nm and

dx.doi.org/10.1021/la402478h | Langmuir 2013, 29, 12663−12669

thickness of t = 1.5 nm, which is very close to the value obtained using the ultrasound measurements discussed above. The median size of the higher mode of the bimodal PSD fit, d_2, corresponds to aggregates of several tactoids that exist in suspension because of the incomplete disintegration of the clay powder. These results confirm the feasibility of using ultrasound attenuation spectroscopy in the study of aging aqueous clay suspensions.

In powder form, Laponite clay comprises big clusters of tactoids. Upon dispersion in water, most of the clusters hydrate and disintegrate into smaller entities. The disintegration of the big tactoids happens due to the absorption of water in the successive monolayers, which, in turn, hydrates the sodium ions between a pair of platelets. The osmotic pressure of the hydrated sodium ions pushes the platelets apart in a process that leads to the absorption of more water layers. Finally, the screened Coulombic repulsions that develop between the platelets overcome the intraplatelet van der Waals attractions, resulting in further exfoliation. As a new smaller tactoid is produced, the hydrated sodium ions distribute around the exposed negatively charged surfaces, forming diffuse layers that extend into the bulk water phase. The effective volume of each particle increases several times due to the presence of these electrical double layers.

It should be noted here that the fragmentation of clay particles is very fast during the initial stages of the stirring process. As the breakup process results in a build-up of strong intertactoid repulsions, the subsequent fragmentation becomes slower with time. The evolution of PSDs with t_w after the preparation of 3% w/v Laponite suspensions is shown in Figure 4. All the PSDs here are obtained from fits to bimodal

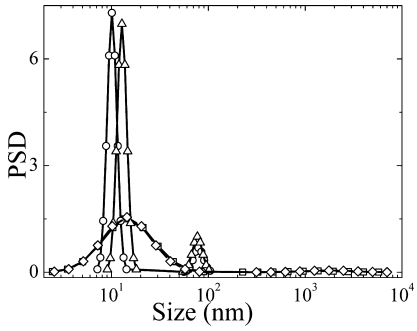

Figure 4. Bimodal size distributions of aggregates in 3% w/v Laponite suspension of t_w = 0 (◊), 3 (□), 4 (○), and 58 (△) h.

distributions. For $t_w \leq 3$ h, the distributions (data points are denoted by □ and ◊) show the presence of some big aggregates (ϕ_2 = 4%) that measure a few micrometers, while the rest of the aggregates are distributed around a median size d_1 of 15 nm but are widespread in size. We estimate the aggregate size in the lower mode by employing graphical solutions of eq 8 and find that this mode is populated by tactoids composed of three to four tactoids. However, as indicated by the broad distributions of the lower modes of the PSDs, tactoids with more than four platelets could be present. At higher ages, most of the bigger aggregates are fragmented into smaller aggregates, and there is the clear emergence of a higher mode of median size d_2 = 80 nm and ϕ_2 = 9%. The remaining tactoids have median size d_1 of 10 nm at t_w = 4 h (○ in Figure 4). At this stage, the lower mode shows a very narrow distribution of sizes and most of the tactoids are composed of one to two tactoids, as estimated before. As the sample ages, the size d_1 in the lower mode increases very slowly. This can be seen from the distribution at t_w = 58 h (△). Since the recoagulation of clay platelets are prevented due to strong repulsions, the increase in particle sizes could be due to the slow absorption of one or two layers of water by the tactoids comprising more than one platelet. The complete exfoliation of most of these swollen tactoids are prevented as the intertactoid repulsions are much stronger than the intratactoid repulsions. A slow growth of the intertactoid repulsions has been indicated in a previous study using X-ray photon correlation spectroscopy.[33] Such an increase in the repulsive force with suspension age explains the ergodic to nonergodic transition observed frequently in experiments on Laponite suspensions of concentrations above 2% w/v.[2] The slow exfoliation of tactoids after sample preparation releases intercalated Na^+ ions into the bulk water. This contributes to an increase in suspension conductivity with age of the clay suspension and has been observed in a previous study.[34]

Acoustic measurements are repeated in three other Laponite concentrations: 1.5%, 2%, and 4% w/v. The major contribution to ultrasound attenuation is consistently seen to arise from the particles in the lower modes of the distributions. The evolutions of the attenuation coefficients α at a frequency of 66.3 MHz and the lower median size d_1 with t_w for all four different concentrations are shown in Figure 5 (panels a and b),

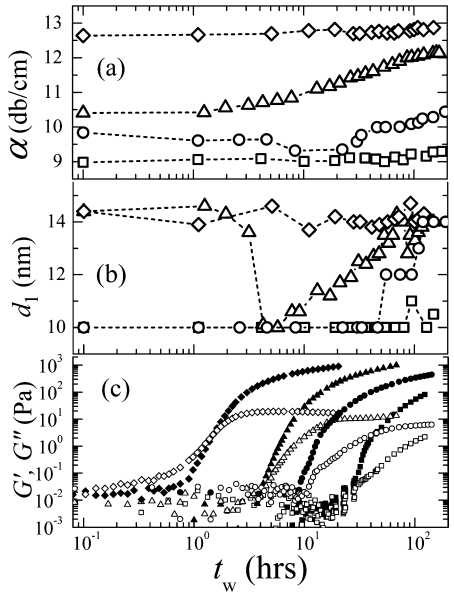

Figure 5. Evolutions of (a) the attenuation coefficient α at an ultrasound frequency of 66.3 MHz, (b) the median sizes d_1 and (c) the elastic moduli G' (solid symbols) and the viscous moduli G'' (open symbols) with age t_w for 1.5% w/v (□), 2% w/v (○), 3% w/v (△), and 4% w/v (◊) Laponite suspensions. For rheological measurements, oscillatory shear strains of amplitude γ_0 = 0.5% at an angular frequency of ω = 1 rad/s were applied.

respectively. Even at other applied frequencies in the range of 10−99.5 MHz, the trends reported below are repeated. Due to the slow exfoliation and the swelling of the tactoids described earlier, the attenuation for the 3% w/v suspension (△) increases slowly over time and shows an approximately 16% increase before finally saturating. The 2% w/v sample (○) shows an increase in the attenuation coefficient α and a lower

dx.doi.org/10.1021/la402478h | Langmuir 2013, 29, 12663−12669

mode median size d_1 at a much later age when compared to the 3% w/v sample. The other two samples of concentrations 1.5% w/v (□) and 4% w/v (◇) do not show any substantial change in α, with d_1 values remaining nearly constant at 10 and 14.6 nm, respectively. As the free volume in the 1.5% w/v suspension is quite large, most of the clusters break down to single platelets during the stirring period and a steady state is easily reached. This explains the constant values of α and d_1 for the 1.5% w/v suspension. On the other hand, the clusters in the 4% w/v suspension disintegrate into tactoids composed of two to three platelets during stirring, following which the suspension rapidly undergoes kinetic arrest due to the highly repulsive interactions between the tactoids. In this case, the intertactoid repulsions, which are much higher than the intratactoid repulsions, prevents further swelling and disintegration. This is clearly observed in Figure 5 (panels a and b). The enhancement of the intertactoid repulsions as a result of the exfoliation of the tactoids is confirmed qualitatively with the age-dependent viscoelastic responses of the Laponite suspensions. The evolutions of elastic modulus G' (solid symbols) and viscous modulus G'' (empty symbols) with t_w for different concentrations are shown in Figure 5c. Soon after preparation, the 4% w/v Laponite suspension (◇) begins to show a predominantly elastic response which indicates a jammed state. With aging, both the moduli increase rapidly by several decades due to microscopic rearrangements and the sample finally exhibits a predominantly elastic response. The 3% w/v suspension (△) starts exhibiting a viscoelastic response at an age where the median size of particles drops to a minimum value (Figure 5, panels b and c). The origin of kinetic arrest in the 1.5% w/v Laponite suspension (□) exhibited at very large ages cannot be related to the repulsion-induced jamming behavior, as there is no change in tactoid sizes (□ in Figure 5b). It has been mentioned earlier that a Laponite platelet contains weak positive charges on its rim.[2] The kinetic arrest in 1.5% w/v suspension can be attributed to the formation of house-of-cards structures (gels) due to the presence of face−rim attractive interactions between the suspended Laponite particles.

IV. CONCLUSIONS

In this work, the exfoliation process of highly anisotropic particles of Laponite and Na-montmorillonite clays in aqueous suspensions is studied using ultrasound attenuation spectroscopy (UAS). As the aggregate sizes are smaller than the acoustic wavelength used, the calculated theoretical loss fits well to the experimental data considering only the visco-inertial interactions. The PSDs are extracted by modeling the data, using bimodal distributions. The number of platelets per tactoid is estimated using an ESD formula proposed in ref 28. Our analysis confirms the presence of tactoids that consist of more than one platelet in Laponite suspensions of concentrations between 1.5% and 4% w/v. The viscous attenuation for concentrations below 1.5% w/v is very small and becomes comparable to the noise of measurement of the intrinsic attenuation. This results in difficulty in data analysis. Some earlier studies using SAXS, DLS, and AFM have demonstrated the presence of tactoids comprising more than one platelet in aqueous Laponite suspensions of concentrations less than 1.5% w/v.[8−11] A transient electrically induced birefringence (TEB) study on Laponite RD suspensions has also indicated an increase in the average tactoid size with volume fraction of clay particles in the concentration range of 0.1−0.8% w/v.[12] However, at very low concentration (0.025% w/v was studied in ref 13), aggregates are found to quickly disperse into individual discs. The data from these previous studies, along with the results obtained from the ultrasound spectroscopy experiments reported here, indicate that the tactoid size distributions in aqueous suspensions of clay depend on the concentration of clay particles. The time evolution of PSDs in a 3% w/v Laponite suspension indicates that the polydispersity of tactoid sizes decreases substantially with age. The same behavior can also be observed in a 3% w/v aqueous suspension of Na-montmorillonite (Figure S7 of the Supporting Information). The age evolution of the ultrasound attenuation coefficient α (and hence the PSDs) for different clay concentrations indicate a major role of electrostatic interactions in the tactoid exfoliation process. During the aggregate dispersion process, when the intertactoid repulsions becomes comparable to the intratactoid repulsions, further exfoliation of the tactoids into smaller entities becomes very slow. We believe that this is the main reason behind the incomplete disintegration of clay clusters in the concentration range studied here. Our study therefore justifies our claim that UAS is a useful technique to elucidate the PSDs of colloidal suspensions, whose concentrations lie in a range where other techniques, like DLS or AFM, often fail.

■ ASSOCIATED CONTENT

Supporting Information

AFM images of Laponite tactoids and the estimation of the sizes and the thicknesses of the tactoids are shown in Figures S1 and S2. A plot verifying the Beer−Lambert law (Figure S3), supplied values of different constants used in eq 3, the method of graphical solutions (Figure S4), AFM image analyses of Na-montmorillonite tactoids (Figures S5 and S6), and a plot for age evolution of aggregate sizes of Na-montmorillonite in aqueous suspension (Figure S7) are provided. This material is available free of charge via the Internet at http://pubs.acs.org.

■ AUTHOR INFORMATION

Corresponding Author

*E-mail: samim@rri.res.in; ranjini@rri.res.in.

Notes

The authors declare no competing financial interest.

■ ACKNOWLEDGMENTS

The authors thank Dr. A. Dukhin for useful discussions and Mr. A. Dhason for his help in acquiring AFM images.

■ REFERENCES

(1) Kroon, M.; Vos, W. L.; Wegdam, G. H. Structure and formation of a gel of colloidal discs. *Phys. Rev. E* **1998**, *57*, 1962−1970.

(2) Ruzicka, B.; Zaccarelli, E. A fresh look at the Laponite phase diagram. *Soft Matter* **2011**, *7*, 1268−1286.

(3) Jabbari-Farouji, S.; Zargar, R.; Wegdam, G. H.; Bonn, D. Dynamical heterogeneity in aging colloidal glasses of Laponite. *Soft Matter* **2012**, *8*, 5507−5512.

(4) Bonn, D.; Tanase, S.; Abou, B.; Tanaka, H.; Meunier, J. Laponite: Aging and shear rejuvenation of a colloidal glass. *Phys. Rev. Lett.* **2002**, *89*, 015701.

(5) Laponite Additives: Synthetic Silicate Additives. http://www.laponite.com (accessed Dec 10, 2012).

(6) Southern Clay Products, Inc.: Rockwood Additives Limited. http://www.scprod.com (accessed Dec 10, 2012).

(7) Joshi, Y. M. Model for cage formation in colloidal suspension of Laponite. *J. Chem. Phys.* **2007**, *127*, 081102.

(8) Thompson, D. W.; Butterworth, J. T. The nature of Laponite and its aqueous dispersions. *J. Colloid Interface Sci.* **1992**, *151*, 236−243.
(9) Saunders, J. M.; Goodwin, J. W.; Richardson, R. M.; Vincent, B. A Small-angle X-ray scattering study of the structure of aqueous Laponite dispersions. *J. Phys. Chem. B* **1999**, *103*, 9211−9218.
(10) Rosta, L.; Gunten, H. R. V. Light scattering characterization of Laponite sols. *J. Colloid Interface Sci.* **1990**, *134*, 397−405.
(11) Balnois, E.; Durand-Vidal, S.; Levitz, P. Probing the morphology of Laponite clay colloids by atomic force microscopy. *Langmuir* **2003**, *19*, 6633−6637.
(12) Bakk, A.; Fossum, J. O. Viscosity and transient electric birefringence study of clay colloidal aggregation. *Phys. Rev. E* **2002**, *65*, 021407.
(13) Nicolai, T.; Cocard, S. Light scattering study of the dispersion of Laponite. *Langmuir* **2000**, *16*, 8189−8193.
(14) Kroon, M.; Wegdam, G. H.; Sprik, R. Dynamic light scattering studies on the sol-gel transition of a suspension of anisotropic colloidal particles. *Phys. Rev. E* **1996**, *54*, 65416550.
(15) Bonn, D.; Tanaka, H.; Wegdam, G.; Kellay, H.; Meunier, J. Aging of a colloidal "Wigner" glass. *Europhys. Lett.* **1999**, *45*, 52−57.
(16) Ruzicka, B.; Zulian, L.; Ruocco, G. Routes to gelation in a clay suspension. *Phys. Rev. Lett.* **2004**, *93*, 258301.
(17) Jabbari-Farouji, S.; Wegdam, G. H.; Bonn, D. Aging of rotational diffusion in colloidal gels and glasses. *Phys. Rev. E* **2012**, *86*, 041401.
(18) Abou, B.; Bonn, D.; Meunier, J. Aging dynamics in a colloidal glass. *Phys. Rev. E* **2001**, *64*, 021510.
(19) Dukhin, A. S.; Goetz, P. J. *Characterization of Liquids, Nano- and Microparticulates, and Porous Bodies using Ultrasound*, 2nd ed.; Elsevier: New York, 2010.
(20) Strutt, J. W.; Rayleigh, B. *Theory of Sound*; Dover Publication Inc.: New York, 1945; Vol. 2.
(21) Harker, A. H.; Temple, J. A. G. Velocity and attenuation of ultrasound in suspensions of particles in fluids. *J. Phys. D.: Appl. Phys.* **1988**, *21*, 1576−1588.
(22) Gibson, R. L.; Toksoz, M. N. Viscous attenuation of acoustic waves in suspensions. *J. Acoust. Soc. Am.* **1989**, *85*, 1925−1934.
(23) Happel, J. Viscous flow in multiparticle systems: Slow motion of fluids relative to beds of spherical particles. *AIChE J.* **1958**, *4*, 197−201.
(24) Hay, A.; Mercer, D. On the theory of sound scattering and viscous absorption in aqueous suspensions at medium and short wavelengths. *J. Acoust. Soc. Am.* **1985**, *78*, 1761−1771.
(25) Dukhin, A. S.; Parlia, S.; Klank, D.; Lesti, M. Particle sizing and zeta potential of silica koestrosol (basis for certified reference material ERM-FD100 for nanoparticles) by acoustics and electroacoustics. *Part. Part. Syst. Charact.* **2012**, *27*, 165−171.
(26) Ahuja, A. S.; Hendee, D. R. Effect of particle shape and orientation on propagation of sound in suspension. *J. Acoust. Soc. Am.* **1978**, *63*, 1075−1080.
(27) Babick, F.; Richter, A. Sound attenuation by small spheroidal particles due to visco-inertial coupling. *J. Acoust. Soc. Am.* **2006**, *119*, 1441−1448.
(28) Jennings, B. R.; Parslow, K. Particle size measurement: The equivalent spherical diameter. *Proc. R. Soc. Lond. A* **1988**, *419*, 137−149.
(29) Avery, R. G.; Ramsay, J. D. F. Colloidal properties of synthetic hectorite clay dispersions: II. Light and small angle neutron scattering. *J. Colloid Interface Sci.* **1986**, *109*, 448−454.
(30) Bonn, D.; Kellay, H.; Tanaka, H.; Wegdam, G.; Meunier, J. Laponite: what is the difference between a gel and a glass? *Langmuir* **1999**, *15*, 7534−7536.
(31) Zhivkov, A. M.; Stoylov, S. P. Electro-optical characterization of aqueous Laponite suspensions. *Colloids Surf., A* **2002**, *209*, 315−318.
(32) Cadene, A.; Durand-Vidal, S.; Turq, P.; Brendle, J. Study of individual Na-montmorillonite particles size, morphology, and apparent charge. *J. Colloid Interface Sci.* **2005**, *285*, 719−730.
(33) Bandyopadhyay, R.; Liang, D.; Yardimci, H.; Sessoms, D. A.; Borthwick, M. A.; Mochrie, S. G. J.; Harden, J. L.; Leheny, R. L. Evolution of particle-scale dynamics in an aging clay suspension. *Phys. Rev. Lett.* **2004**, *93*, 228302.
(34) Shahin, A.; Joshi, Y. M. Physicochemical effects in aging aqueous Laponite suspensions. *Langmuir* **2012**, *28*, 15674−15686.